EAI Endorsed Transactions
on Energy Web
Research Article EAI.EU

Characterization and Prediction of Wind Turbine Blade Damage Based on Fiber Grating Sensor

Xin Guan[1,a], Qizheng Mu[1,b], Xiaoju Yin[1,c*], Yuxin Wang[2,d*]

[1]Department of Renewable Energy, Shenyang Institute of Engineering, Shenyang, 110136, China
[2]Collage of Computer and Information Engineering, Tianjin Agricultural University, Tianjin, 300387, China

Abstract

INTRODUCTION: As a renewable and clean use of energy, wind power generation has a very important role in the new energy generation industry. For the many parts of various wind turbines, the safety and reliability of wind turbine blades are very important.
OBJECTIVES: The energy spectrum simulation algorithm included in the wavelet analysis method is used to simulate and analyzewind turbine blade damage, to verify the correctness and validity of wind turbine blade damage analysis.
METHODS: Matlab simulation is used to introduce the experiments related to the static and dynamic detection of fiber grating sensors, analyze the signal characteristics of the wind turbine blade when it is damaged by the impact, and provide a basis for the analysis of the external damage of large wind turbine blade.
RESULTS: The main results obtained in this paper are the following. By analyzing the decomposition of wavelet packets, the gradient change of wavelet impact energy spectrum before and after the wavelet damage was obtained and compared with the histogram, and the impact energy spectrum of each three-dimensional wavelet energy packet in the image was compared and analyzed, which can well realize the recognition of wavelet damage gradient for solid composite materials.
CONCLUSION: With the help of Matlab simulation to collect the impact response signal, using the wavelet packet energy spectrum method to analyze the signal, can derive the characteristics of wind turbine blade damage.

Keywords: Wind turbine, wind turbine blade, damage detection, energy spectrum

Received on 19 November 2023, accepted on 07 April 2024, published on 12 April 2024

doi: 10.4108/ew.5752

1. Introduction

Wind energy is one of the fastest-growing renewable energy resources. The blades are regarded as one of the most critical components in a wind turbine[1]. Wind turbine in terms of blade materials used is the combination of various composite materials to form a thin shell blade structure, this composition of the main type of material is usually called glass fiber can also be said to be a reinforced version of glass fiber, the wind turbine blade introduced and analyzed in this paper is composed of glass fiber composite materials[2]. Due to the wind turbine manufacturing production process and other factors, the wind turbine blade in the operation of the power supply service the wind turbine load, and other factors interference and impact, factors will directly lead to the wind turbine blade internal cracks, voids, delamination or debonding and other damage[3-5], so need to take some special detection methods to the wind turbine blade implementation of strict testing.

The detection can use the detection method of ultrasound, x-ray inspection method, computerized chromatography detection method, microwave detection method, ultrasound detection method, and acoustic emission detection method[6]. The robust principal component analysis method is used to preprocess the blade image with surface dirt, and the damage feature extraction process is transformed into a convex optimization problem for solving and obtaining the blade damage features[7]. Proposing a thermal infrared image-based method for wind turbine blade damage identification, damage location determination and damage size calculation[8]. The detection method of computerized

[a]xinguan@sina.com, [b] 905105393@qq.com, [c*]Corresponding authors: lnsolyxj@163.com, [d*]261235654@qq.com

laminography has a better spatial resolution, as well as density resolution, a higher density in terms of imaging size, a larger range of dynamics that can be detected, a more intuitive three-dimensional image detected, and the geometry, is unrestricted at sufficient penetration energy, but the cost of this method is relatively high, low efficiency, and the double side will be transmissive imaging, so it is not applicable in large components and components of flat thin plates. The detection method of ultrasound is more suitable for assessing the integrity of materials, but its signal-to-noise is relatively low, and it is more difficult to extract useful signals. A material damage identification model combining principal component cluster analysis and BP neural network is proposed based on acoustic emission technology. It has a better ability to recognize the unknown damage[9]. Construction of an attenuated sinusoidal and exponential wavelet threshold function for noise reduction of acoustic emission signals with low signal-to-noise ratio[10]. The detection method of acoustic emission can obtain the defects and damage that the composite material has, and in its development, because of the rich and active amount of information, this technique can be applied to more advanced production and research and development, playing a very important role, but it also has certain disadvantages, making it difficult to distinguish between signal and noise[11]. Existing passive acoustics-based techniques for wind turbine blade damage detection lack the robustness and adaptability necessary for an operational implementation due to their physics- and model-based dependency[12].

This paper studies the method of detecting whether the blade of a wind turbine has damage based on a fiber grating sensor[13]. The volume and mass of the fiber grating sensor are relatively small, with strong anti-interference ability, which has certain advantages in many detection methods, so this detection method is commonly applied to the process of detecting the blade of the wind turbine. Further studies found that ultrasonic sensors using fiber grating to detect fatigue cracks in metals are more sensitive to ultrasonic waves and can locate the tip of the crack [14,15].

In this paper, the fiber grating sensor is used for the dynamic experiment of the blade, and Matlab is used to simulate the vibration experiment[16], the impact experiment is conducted by the relationship between the waveform of the output signal of the fiber grating sensor and the placement distance and placement angle of the sensor, and the relationship between the impact signal and the placement position of the sensor is sought [17,18].

The gradient change of the multi-order wavelet impact energy spectrum before and after the damage is compared to the impact energy spectrum of the three-dimensional order wavelet energy packet to realize the wavelet damage gradient identification [19,20].

2. Analytical model of the coupled-mode theory of fiber grating

2.1. Coupled-mode theory of fiber grating

Coupled-mode theory describes the coupling behavior of optical waves in a more comprehensive and detailed way and is usually used very widely in the quantitative description of fiber gratings, so it is the most fundamental method for analyzing fiber gratings in current studies. The coupled mode equation is obtained with the help of the micro-motion condition of the ideal light wave tube, Maxwell's equation, mode orthogonally, and boundary conditions.

In general application situations, the high-frequency microwave-modulated signal is usually treated as a microwave-type interference, which is generated under the stimulation of microwave UV radiation from the transmitting fiber or adjacent cores. Inside the fiber grating range, the transverse component of the electromagnetic field is considered to be a superposition of many unperturbed ideal modes as in equation (1):

$$E^T(x,y,z,t)=\sum_j\left[A_j(z)\exp\left(i\beta_j z\right)+B_j(z)\exp\left(-i\beta_j\right)\right]e_j^T(x,y)\exp(-iwt) \quad (1)$$

WhereA_j- slow-variant amplitude in j modes flowing along +z direction, B_j- slow-variant amplitude in j modes flowing along -z direction, β_j - transmission constant, e^T_j (x, y) - transverse mode field.

Under the influence and stimulation of the refractive index, when a perturbation occurs, the amplitudes A_j and $B_j$in the jth mode will move in the z direction, and the law of this change moves satisfies the following equation (2) equation (3):

$$\frac{dA_j}{dz}=i\sum_k A_j\left(C_{kj}^T+C_{kj}^z\right)\exp\left[i\left(\beta_k-\beta_j\right)z\right]+i\sum_k B_k\left(C_{kj}^T+C_{kj}^L\right)\exp\left[i\left(\beta_k+\beta_j\right)z\right] \quad (2)$$

$$\frac{dB_j}{dz}=-i\sum_k A_k\left(C_{kj}^T+C_{kj}^z\right)\exp\left[i\left(\beta_k-\beta_j\right)z\right]-i\sum_k B_k\left(C_{kj}^T+C_{kj}^L\right)\exp\left[-i\left(\beta_k-\beta_j\right)z\right] \quad (3)$$

In the two equations listed above, the transverse coupling coefficient C^T_{kj} between the jth and kth modes can be reflected as:

$$C_{kj}^T(z)=\frac{\omega}{4}\int_0^a\int_0^{2\pi}\Delta\varepsilon(x,y,z)e_j^T(x,y)\cdot e_j^T(x,y)\,xdydx \quad (4)$$

Where $\Delta\varepsilon\ (x,y,z)$ - the perturbation of the dielectric constant.

If only the effective refractive index of the wave tube mode is considered to be perturbed, the refractive index distribution of the fiber after UV irradiation is:

$$\delta n_{eff}(z)=\overline{\delta n}_{eff}(z)\left\{1+\upsilon\cos\left[\frac{2\pi}{\Lambda}z+\varphi(z)\right]\right\} \quad (5)$$

Where $\overline{\delta n}_{\text{eff}}$(z)- the average refractive index is changed, υ - the refractive index causes the stripe visibility to be changed, Λ - the grating period, $\varphi(z)$ - the melancholy chirp parameter.

In most fiber gratings, $\overline{\delta n}_{\text{eff}}$(z) is considered to be uniform inside the core, but it is considered to be present outside the core. Therefore, we can use the expression of (5) to express the refractive index of the core, to make its physical meaning clearer, which can be defined as:

$$\sigma_{kj}(z)=\frac{\omega n_{core}}{2}\overline{\delta n}_{core}\int_0^a\int_0^{2\pi}e_j^T(x,y)\cdot e_j^{T*}(x,y)\,xdydx \quad (6)$$

$$k_{kj}(z)=\frac{\upsilon}{2}\sigma_{kj}(z) \tag{7}$$

Based on the above equation, it can be written that equation (5) can be written as:

$$C_{kj}^{T}(z)=\sigma_{kj}(z)+2k_{kj}(z)\cos\left[\frac{2\pi}{\Lambda}z+\varphi(z)\right] \tag{8}$$

Where $\sigma_{kj}(z)$- is the self-coupling coefficient, $C_{jk}(z)$- is the cross-coupling coefficient.

2.2. Fiber grating sensor sensing principle

Fiber optic (Bragg) grating (FBG) is a reflection type of grating that takes the UV-sensitive properties carried by the doped fiber itself and exploits them by irradiating a spatially periodic strong UV laser beam in the doped fiber, thus allowing the core refractive index to follow the axial direction and periodically distribute the reflection conditions.

2.3. Static characteristics of fiber grating sensors

The relationship between the input of a sensor and its output is mostly non-ideal for non-linear sensors, so we can use this polynomial to represent the relationship between the input and its output in a sensor:

$$Y=f(x)=b_0+b_1X^1+b_2X^2+\ldots+b_nX^n \tag{9}$$

Where X - input signal, Y - output signal, b_0 -zero output, b_1- linear and sensitivity, b_2、b_3....b_n, - sensor nonlinearity coefficient.

However, in the case of characteristic curves where the input-output relationship of the sensor is already known, the coefficients of binomial (b2) and above binomial (bi(i> 2))can be ignored as zero. The linear accuracy equation for this type of sensor can be expressed in Equation (10) as follows:

$$\delta L=\pm\frac{\Delta L_{\max}}{Y_{FS}} \tag{10}$$

Where δL - the linearity of the sensor, Y_{FS} - the full-scale output of the sensor, $\triangle L_{max}$ - the maximum deviations of the calibration curve and the fitted curve of the sensor.

3. Simulation analysis calculation

3.1. Vibration calculation for composite plates

The composite substrate consists of many single-layer sheets spliced together. Since the single-layer sheets are very thin, after being bonded, the total thickness of the composite is also very thin, and its thickness is much smaller than the deflection, and we can regard the composite sheet as anisotropic. To study the vibration equation of the composite material in depth, the coordinate system should be set up first, with the length extension direction of the composite plate set as the x-axis, the width extension direction as the y-axis, and the thin thickness direction as the z-axis. Following the invariant assumption method of the linear method and the integral method, we can express the displacement components of all points on the composite plate:

$$\begin{cases} w(x,y,z)=w_0(x,y) \\ u(x,y,z)=u(x,y)-z\dfrac{\partial w_0(x,y)}{\partial x} \\ v(x,y,z)=v_0(x,y)-z\dfrac{\partial w_0(x,y)}{\partial y} \end{cases} \tag{11}$$

Where W_0- displacement component of the mid-plane, u_0 - displacement component of the mid-plane, v_0 - displacement component of the mid-plane, w -disturbance function of the system.

The strain component can be obtained from the micro deformation equation as:

$$\begin{cases} \varepsilon_x=\dfrac{\partial u_0}{\partial x}-z\dfrac{\partial^2 w_0}{\partial x^2} \\ \varepsilon_y=\dfrac{\partial w_0}{\partial y}-z\dfrac{\partial^2 w_0}{\partial y^2} \\ \gamma_{xy}=\dfrac{\partial u_0}{\partial y}+\dfrac{\partial v_0}{\partial x}-2z\dfrac{\partial^2 w_0}{\partial x\partial y} \end{cases} \tag{12}$$

Then according to Hooke's law of plane stress, we have:

$$\begin{cases} \sigma_x=\dfrac{E}{1-v^2}(\varepsilon_x+v\varepsilon_y) \\ \sigma_y=\dfrac{E}{1-v^2}(\varepsilon_y+v\varepsilon_y) \\ \tau_{xy}=\dfrac{E}{2(1+v)}\gamma_{xy} \end{cases} \tag{13}$$

The differential equation for the vibration of the composite plate is:

$$\frac{\partial^4 w}{\partial x^4}+2\frac{\partial^4 w}{\partial x^2\partial y^2}+\frac{\partial^4 w}{\partial y^4}+\frac{\rho}{D}\frac{\partial^2 w}{\partial t^2}=\frac{1}{D}F(x,y,t) \tag{14}$$

Where $w(x,y,t)$ - the vibration amplitude,

ρ - mass per unit area,

$F(x,y,t)$- the strength of the load-bearing load that is forced to vibrate,

D - Bending stiffness parameter.

If the bearing load strength of the forced vibration $F(x,y,t)=0$, is in the free vibration state, the differential equation of the vibration is:

$$\frac{\partial^4 w}{\partial x^4}+2\frac{\partial^4 w}{\partial x^2\partial y^2}+\frac{\partial^4 w}{\partial y^4}+\frac{\rho}{D}\frac{\partial^2 w}{\partial t^2}=0 \tag{15}$$

3.2. Test idea

Vibration simulation experiments were conducted for the composite materials during excitation. Seven fiber-optic grating sensors were attached to the sheet, and they were named FBG1-FBG7. The positions of the sensors and their naming numbers are shown in Fig.1 where the sensor FBG1 is affixed to a length of 50 mm from the excitation position of

the shaker extending along the x-axis, sensor FBG2 is pasted at a length extending 20 mm along the x-axis from the position of sensor FBG1, sensor FBG3 is attached at a distance of 50 mm from the excitation position of the shaker along the x-axis, sensors FBG4 and FBG3 are pasted at 90 degrees to each other, sensor FBG5 is attached to the sheet made of composite material at an angle of 30° to sensor FBG3, sensor FBG6 is pasted at a distance of 100 mm from the excitation position on the sheet formed by the composite material extending in the negative direction along the x-axis, and sensor FBG7 is attached at a distance of 80 mm from the excitation position of the exciter on the sheet made of composite material extending along the negative direction of the x-axis.:

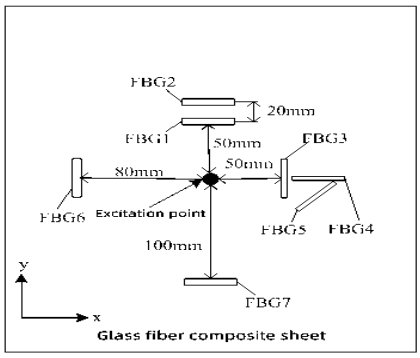

Figure 1. Vibration experiment simulation diagram

In the vibration simulation experiment of the vibration simulation of composite materials, using Matlab wavelet simulation and then filtered by the filter in the wavelet toolbox, by imitating the direct observation of Fig.2 can be seen that the difference between the original signal map of the two sensors and their original signal map after filtering is not very obvious, there is no way to conclude the comparison, so the frequency domain signals of the two sensors are compared here.

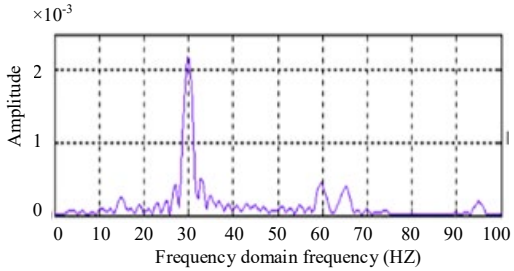

(a) Frequency domain amplitude of sensor 1

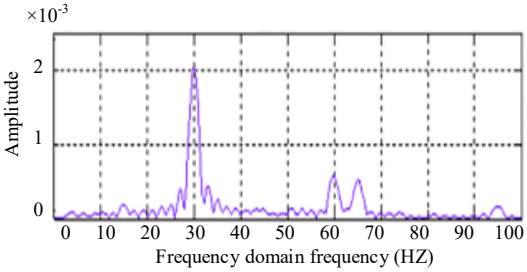

(b) Frequency domain amplitude of sensor 2

Figure 2. Frequency domain signal comparison char.

This conclusion is obtained by comparing the frequency domain signals of the sensors: the frequency domain amplitude of sensor1 is greater than the frequency domain amplitude of sensor2 at a frequency of 30 Hz, so the excitation signal received by the sensor must be related to the distance of the sensor affixed to the sheet from the excitation point located on the composite material.

3.3. Wavelet packet energy spectrum for impact response damage identification

A simple impact test was performed on a fiberglass composite panel to test the effectiveness of such an initiative with a small wave packet energy spectrum. A glass fiber composite plate is fixed to the experimental table, which has the property of being optically shockproof, and then a fiber grating sensor is placed on the surface. In this simulation, an impact hammer was used to strike a thin plate made of glass fiber composite material with a determined amount of 0.15 J, and displacement loads of 1 mm, 3 mm, and 5 mm were applied at the locations of the simulated loading damage. A simulated experimental sheet composed of composite materials without any displacement load applied, with a 1 mm displacement load applied, with a 3 mm displacement load applied, and with a 5 mm displacement load applied was struck. The time domain signal of the shock obtained after simulation is shown in Fig.3:

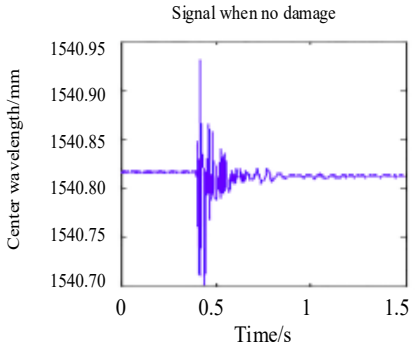

(a) No displacement load

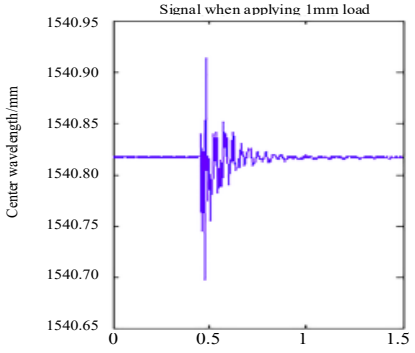

(b) Apply 1 mm displacement load

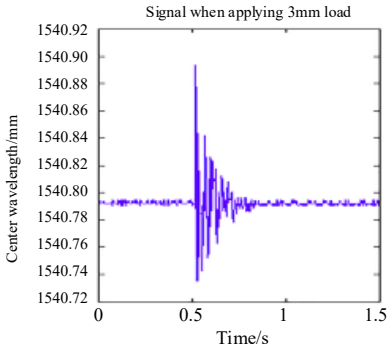

(c) Apply a 3 mm displacement load

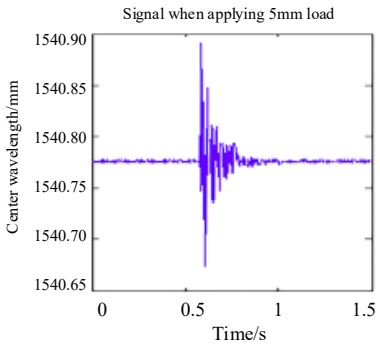

(d) Apply a 5 mm displacement load

Figure 3. Time-domain signal at impact

The time domain signals of the simulated experimental sheet composed of composite materials when subjected to impact can be derived from Fig.3 in the absence and presence of damage. However, because the time domain signals are so dense, it is very difficult for us to conclude from these four-time domain signal maps whether they carry damage or not. Therefore, the waveform plots out of which 1 mm displacement load, 3 mm displacement load, and 5 mm displacement load were applied were decomposed into wavelet packet energy spectra respectively, and then compared with the wavelet packet energy spectra of each order when there were no damage, the changes of the energy spectra of the 10th and 23rd orders were very large, so that when there was a breakage in the wind turbine blade material, it led to a change in the values of the parameters of that material, etc., which led to an increase in the changes than the wavelet packet energy spectra of the 10th and 23rd orders respectively. This change is more prominent when the wind turbine blade material is more severely damaged, and by this conclusion, it can be concluded that the use of the wavelet packet energy spectrum method can detect the damage of this material.

3.4. Simulation of existing data using MATLAB

The data is mainly from the wind farm, all the data will be created variables, the sensors will be simulated and simulated to lose open the wavelet toolbar; select the wavelet packet tool and open to derive the fitted curve. The waveform of the output sensor is obtained, and the feedback signals of the six sensors are derived.

Using different objects pasted on the wind turbine blade to simulate different damages of the blade, the collected data were input again and the damage signal of the wind turbine blade was fitted using Matlab. Since the sensor angle is best when the sensor center point and the line of the impact point are laid vertically, sensor 2 is chosen as the study object for simulation. Import the collected experimental data from Zhangbei wind farm, open the wavelet toolbar of Matlab, select the wavelet packet tool, and after fitting, the waveform output of the sensor after the wind turbine blade is attached to the block is shown in Fig.4:

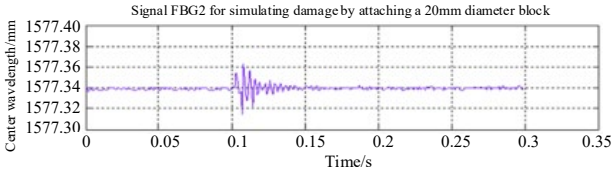

(a) Transmission waveforms of undamaged blades

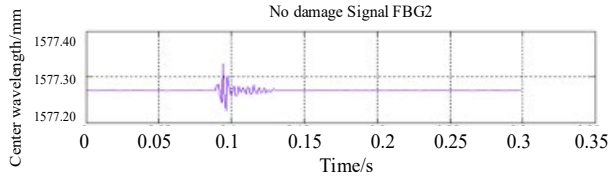

(b) Output signal for 20mm diameter object

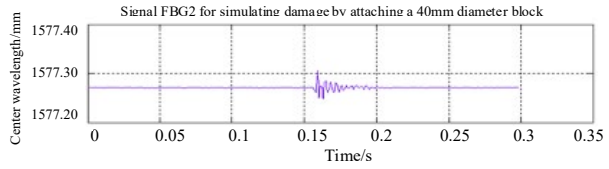

(c) Output signal for 40mm diameter object

Figure 4. Damage analog signal simulation diagram

Run the program can be derived from the wind turbine blade with damage and no damage wavelet packet energy change when the blade is not damaged, the experimental simulation to get the wavelet packet energy spectrum of each order change is relatively small, when the blade damage experimental simulation to get the wavelet packet energy spectrum of each order change is relatively large, in the 11th order and the 27th order of the amount of change is very prominent. From Fig (b) and (c) comparison can be derived from the diameter of the 20mm block in the impact of the 11th and 27th order of change are less than the diameter of the 40mm block, so the larger the damage, the wavelet packet energy spectrum of the 11th and 27th order of change is greater, you can use the wavelet packet energy spectrum method to detect the size of wind turbine blade damage.

4. Discussion

In this paper, a fiber grating sensor is used to detect whether the blade is lost or not, and an energy spectrum simulation method using wavelet analysis is proposed to simulate the blade damage. The method analyzes the influence of the position of the fiber grating sensor on the detection, and analyzes the characteristics of the time-domain and frequency-domain signals at the time of blade failure. The results show that the method can recognize and extract the damage characteristics of the blade. The method can be applied to wind turbine blade damage identification.

Although this paper verifies the effectiveness and accuracy of the method. However, the fiber grating sensor is particularly sensitive to ultrasonic waves, which may lead to misjudgement. n the future, more accurate and more effective algorithms are used in conjunction.

5. Conclusion

(1)Three different coupling modes of fiber grating sensors have been analyzed and studied in terms of coupling multiplexing techniques: time division multiplexing, coupling multiplexing of space division, and coupling multiplexing of central wave division.

(2) The main blade body structure that we want to study is a composite material of glass fiber. Matlab was used to simulate vibration experiments, and the relationship between the waveform of the output signal of the fiber grating sensor and the placement distance and placement angle of the sensor could be obtained. Impact experiments were conducted and the relationship between the impact signal and the placement of the sensor was obtained. At a frequency of 30 HZ, the amplitude of the frequency domain increases with distance. By analyzing the decomposition of wavelet packets, the gradient change of wavelet impact energy spectrum before and after the wavelet damage was obtained and compared with the histogram, and the impact energy spectrum of each three-dimensional wavelet energy packet in the image was compared and analyzed, which can well realize the recognition of wavelet damage gradient for solid composite materials.

(3) A wind turbine blade simulation diagram was constructed to simulate the state of the external surface of the wind turbine blade being destroyed, and the impact response signal was collected with the help of Matlab simulation, and the signal was analyzed by using the wavelet packet energy spectrum approach to derive the characteristics of the wind turbine blade when it was damaged.

Acknowledgements.

China University Innovation Fund -- New Generation Information Technology Innovation Key Project, No. 2022IT017; Education Reform Project of China Institute of Labor Electronics in 2022, No.CIEL2022060; Cooperative Education Program of Ministry of Education, No.220900287260151, No.202102602013; Key Project of Graduate Education and Teaching Research and Reform of Tianjin Agricultural University, No. 2021-YA-6; Talent Support Program of Tianjin Agricultural University, No. Y0400907; School-enterprise cooperation technology research and development project (TNHXKJ2022074, TNHXKJ2023009).

Tianjin Graduate Research Innovation Program, No.2022Skyz258, 2022SKYZ261. Natural Science Foundation of Liaoning Province (2022-MS-305) Foundation of Liaoning Province Education Administration (LJKZ1108).

References

[1] Li, X. Few-shot wind turbine blade damage early warning system based on sound signal fusion. Multimedia Systems 29, 2913–2922 (2023).

[2] Rani Manjeet et al. Development of sustainable microwave-based approach to recover glass fibers for wind turbine blades composite waste. Resources, Conservation & Recycling, 2022, 179.

[3] Dietmar, Tilch, Daniel, et al. Condition Monitoring of Rotor Blades:Damages, ICe, Overload //The 13th World Wind Energy Conference(WWEC2014). 2014:1-8,52.
[4] Jihong Guo. Research on damage detection of fan blades based on computer vision and deep learning algorithm. Qingdao University of technology, 2021 DOI:10.27263/d.cnki. gqudc. 2021.000144.
[5] Jian Dong. Research on fault early warning and life assessment method and its application of key components of wind turbine. North China Electric Power University (Beijing), 2021 DOI:10.27140/d.cnki. ghbbu. 2021.000126.
[6] Gongtian Shen. Development status of non-destructive testing and evaluation technology for pressure equipment. Journal of mechanical engineering, 2017, 53 (12):1-12.
[7] LIN Feng, GUO Peng, LIU Xubin. Wind Turbine Blade Surface Damage Identification Based on Blade Surface Dirt Pre-treatment and CNN. Journal of Chinese Society of Power Engineering. 2020, 40(12):975-981.
[8] Yu Y, Yong Z, Jian W, et al. Research on Wind Turbine Blade Damage Identification Method Based on Thermal Infrared Image. Acta Energiae Solaris Sinica, 2022, 43(2):492.
[9] Jia Hui, Zhang Leian, Wang Jinghua, et al. Damage pattern recognition of wind turbine blade composite material based on acoustic emission technology. Renewable Energy Resources, 2022, 40(01):67-72. DOI:10.13941/j.cnki.21-1469/tk.2022.01.008.
[10] YU Yang, LI Yun, YANG Ping, et al. Improved wavelet threshold function and ACEWT method for feature extraction of acoustic emission signals from rolling bearing faults. Journal of Vibration and Shock. 2023, 42(17):194-202.DOI:10.13465/j.cnki.jvs.2023.17.025.
[11] Changing Yang, Luping Li. Research progress of wind turbine blade damage fault detection technology. Power generation technology, 2020,41 (06): 599-607.
[12] Solimine J, Inalpolat M. An unsupervised data-driven approach for wind turbine blade damage detection under passive acoustics-based excitation. Wind Engineering. 2022;46(4):1311-1330.
[13] Pingyu Zhu et al. Reliable packaging of optical fiber Bragg grating sensors for carbon fiber composite wind turbine blades. Composites Science and Technology, 2021, : 108933-.
[14] Xiaohong Bai. Design, fabrication and performance optimization of fiber Bragg grating ultrasonic sensor. Northwestern University, 2021 DOI:10.27405/d.cnki. gxbdu. 2021.002187.
[15] Zhaohui Zhang Wind turbine structure state evaluation method based on optical fiber sensing technology. Harbin Institute of technology, 2020 DOI:10.27061/d.cnki. ghgdu. 2020.004670.
[16] Lihua Yu, Changsheng Chen, Shulong Liu, et al. Using MATLAB software to simulate vibration experiment. College physics experiment, 2011,24 (3):79-81 DOI:10.3969/j.issn. 1007-2934.2011.03.024.
[17] Sayed Ahmed Zaki Ahmed. Photovoltaic system fault detection and diagnosis method based on intelligent algorithm. North China Electric Power University (Beijing), 2021 DOI:10.27140/d.cnki. ghbbu. 2021.000136.
[18] Muhammad Abubakar. Effective detection and classification of multiple power quality disturbances based on statistical parameters and deep learning. Jiangsu University, 2020 DOI:10.27170/d.cnki. gjsuu. 2020.000526.
[19] Contents and Abstracts of Journal of Mechanical Engineering. Chinese Journal of Mechanical Engineering, 2010, 23(01):135-158. Vol.46, No.1 ~ 4, 2010.
[20] Contents and Abstracts of Journal of Mechanical Engineering. Chinese Journal of Mechanical Engineering, 2009, 22(05):772-790. ISSN 0577-6686,CN 11-2187/TH.